Molecular Therapy
Oncology
Original Article

Metabolites and metabolic pathway reactions links to sensitization of immunotherapy in pan-cancer

Shaobo Yu,[1,2,4] Yuzhen Gao,[1,2,4] Feng Zhao,[1,2,4] Jiaqiang Zhou,[3] and Jun Zhang[1,2]

[1]Department of Clinical Laboratory, Sir Run Run Shaw Hospital of Zhejiang University School of Medicine, Hangzhou 310016, Zhejiang, China; [2]Key Laboratory of Precision Medicine in Diagnosis and Monitoring Research of Zhejiang Province, Hangzhou 310016, Zhejiang, China; [3]Department of Endocrinology, Sir Run Run Shaw Hospital, Zhejiang University School of Medicine, Hangzhou 310016, Zhejiang, China

Metabolic features are crucial in tumor immune interactions, but their relationship with antitumor immune responses is not yet fully understood. This study used Mendelian randomization analysis to identify the causal relationships between blood metabolites and immune cells and to evaluate the effects of metabolic pathways and reactions on antitumor immune responses in various cancers. Levels of 156 metabolites exhibited significant associations with selected immune cells. Metabolic enrichment analysis indicated laurate, propionyl-carnitine, carnitine and L-acetylcarnitine are enriched in fatty acid (FA) metabolism pathways. These enriched pathways are significantly correlated to CD8$^+$ T cell function signatures in tumor environment and favor better prognostic outcomes. Metabolic reactions contributing to better immunotherapy responses were identified and used to establish the immuno-metabolic reaction score (IMRS). IMRS were significantly correlated to CD8$^+$ T cell infiltration levels and CD8$^+$ T cell signature scores in either 10× Visium spatial transcriptomic or RNA-seq samples. Finally, IMRS could significantly predict favorable survival outcomes in different cancer patients treated with immunotherapy. Our study revealed a link between certain metabolites and their related metabolic pathways to tumor immune landscape and immune functions. These results could promote the accurate stratification of patients before treatment and improve the efficacy of immunotherapy.

INTRODUCTION

Metabolic reprogramming is a key hallmark of cancer. Tumor cell metabolism modifies the composition of metabolites in the tumor microenvironment (TME). These metabolites have been increasingly recognized for their impact on the immune cells present in this niche through energy, amino acids, and lipid metabolism pathways.[1] Metabolic barriers, including glucose competition of tumor cells with activated effector T cells and upregulation of ligands on tumor cells that bind to inhibitory receptors on immune cells, would impair the efficacy of anti-cancer immunotherapy.[2] With a growing array of immunotherapies entering clinical practice, it remains necessary to assess mechanisms that could shed light on how they might be influenced by immune-metabolic effects.[2,3] Given the intricacies and rapid fluctuations in metabolite concentrations and distributions, there are still many difficulties in pinpointing specific relationships between metabolites and the immune landscape in the TME.

Various immune cells in the TME are crucial for antitumor immunity, but they are inevitably influenced by the metabolic products within this niche. CD8$^+$ T cells, which are responsible for the adaptive immune response, specialize in recognizing and eliminating malignant cells. A recent study revealed that tumor-derived D-2-hydroxyglutarate (D-2HG) is taken up by CD8$^+$ T cells, disrupting their metabolism and impairing their cytotoxicity and interferon-γ signaling in the TME. The impaired functions of CD8$^+$ T cells can be restored by removing immunosuppressive D-2HG from the TME using mutation-specific isocitrate dehydrogenase inhibitors.[4] Other immune cells in the TME, such as tumor-associated macrophages (TAMs), accumulate 25-hydroxycholesterol, which enhances their immunosuppressive functions by activating 5′ AMP-activated protein kinase-α via the GPR155-mammalian target of rapamycin complex 1.[5] Furthermore, metabolites derived not only from tumors *in situ* but also from the gut microbiota can modulate immune cell functions in the TME via systemic circulation.[6] Jia et al. reported that *Lactobacillus johnsonii* collaborates with *Clostridium sporogenes* to produce indole-3-propionic acid, which could facilitate the generation of progenitor exhausted CD8$^+$ T cells by increasing H3K27 acetylation at the super-enhancer region of Tcf7.[7] While these studies provide valuable insights into utilizing metabolic targets to enhance cancer treatment via immunotherapy, they require extensive experimentation and the screening of large clinical sample sets using omics approaches. A more efficient approach is required to promptly identify potential associations and rapidly narrow down the scope of candidate metabolites.

Received 29 August 2024; accepted 10 January 2025;
https://doi.org/10.1016/j.omton.2025.200933.

[4]These authors contributed equally

Correspondence: Jun Zhang, Department of Clinical Laboratory, Sir Run Run Shaw Hospital, Zhejiang University School of Medicine, Qingchun East Road, Jianggan District, Hangzhou 310016, China.
E-mail: jameszhang2000@zju.edu.cn

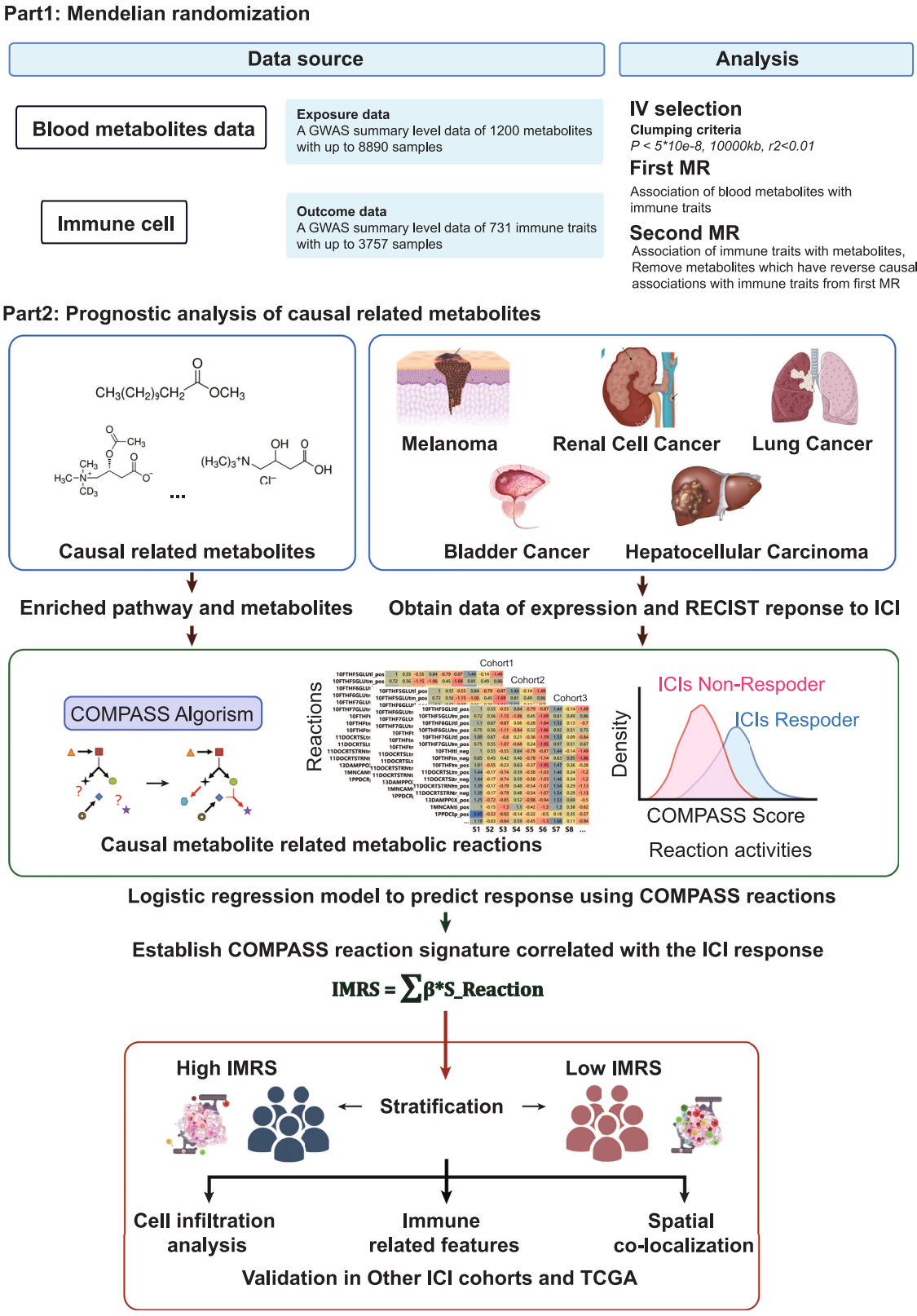

(legend on next page)

The concentration and composition of metabolites in the bloodstream are known to be highly dynamic. The causal effects of these metabolites on immune system modulation, particularly in immune cells, remain an unresolved issue in the field.[8] As the proportion of immune cells is a direct indicator of cancer immunotherapy response,[9] many tools have been developed to analyze TME cell proportions and their relation to prognosis or tumor immunotherapy outcomes, such as TIME2, CIBERSORT, MCP-counter, EPIC, and Estimate.[10] Therefore, establishing the causal relationship between blood metabolites and immune cells is critical for precise patient segmentation and personalized immune interventions. Mendelian randomization (MR) provides an opportunity to distinguish causal and noncausal effects from cross-sectional data, without the need for randomized controlled trials.[11] Recently, a study used MR to identify causal relationships between blood metabolites and seven cancer types, revealing that lipids are particularly causally associated with colorectal cancer (CRC).[12] Moreover, a comprehensive peripheral blood immunoprofiling study developed a signature score based on blood cell RNA sequencing (RNA-seq) and immune cell profiles; the score is correlated with the immunotherapy response across multiple cancer types.[13] In the present study, we hypothesize that the causal relationship between blood metabolites and key immune cells could reflect the immune cell landscape in the TME. These metabolites and the activities of related reactions may serve as prognostic predictors for immunotherapy efficacy.

RESULTS

MR causal relationship of metabolites to immune cells

As outlined in the study scheme (Figure 1), the MR results for all selected immune cells are summarized (see also Table 1). Functional analysis of single-nucleotide polymorphisms (SNPs) selected as instrument variables were revealed. These SNPs are correlated to metabolic pathways such as the carboxylic acid metabolic process, biological oxidation, transport of small molecules, organic anion transport, and the lipid catabolic process (Figure 2A). After MR analysis, 156 metabolites have at least 2 causal relationships with blood immune cells and were considered immune-related metabolites (IRMs) (Figure 2B). These metabolites were subject to pathway enrichment analysis, which indicated that these IRMs enriched in 4 metabolic pathways significantly (adjusted $p < 0.05$). Within these pathways, β-oxidation of very-long-chain fatty acids (BOVLCFAs) and oxidation of branched chain FAs (OBCFAs) both belong to the FA oxidation (FAO) pathways that are most significantly enriched (Figure 2C). These enriched IRMs are laurate (C12), propionyl-carnitine, carnitine, and L-acetylcarnitine (Figure 2D). Causal MR analysis revealed that these IRMs may have causal effects on B cells, myeloid-derived suppressed cells (MDSCs), CD4 regulatory T cells (Tregs), and natural killer T (NKT) cells (Figure 2E).

Effects of FAO pathways on tumor immune interaction

A prediction model of immunotherapy efficacy in pan-cancer patients was established using scores from significantly enriched metabolic pathways. Univariate logistic regression and meta-analysis results indicated that higher FAO pathway scores, represented by BOVLCFAs and OBCFAs were associated with better immunotherapy outcomes (hazard ratio [HR] < 1, $p < 0.05$) (Figure 3A). Prediction of metabolic pathway scores for immunotherapy responses varied across cancer types (Figure 3A). For instance, univariate analysis indicates that high OBCFA pathway scores predicted non-response outcomes in hepatocellular carcinoma (HCC) and non-small cell lung cancer patients although these outcomes are insignificant (HR > 1, $p > 0.05$). To investigate the immune cell modulation effects of FAO pathways, scores for these two pathways were applied to correlation analysis with T cell signatures across all datasets. The OBCFA and BOVLCFA pathways were both positively correlated to cytotoxicity in multiple immunotherapy cohorts (Figure 3B). The OBCFA was positively correlated with oxidative phosphorylation, while the BOVLCFA pathway was negatively correlated with exhaustion in certain cohorts (Figure 3B). In the IMvigor210 cohort, glycolysis was negatively correlated with the immune-proficient $CD8^+$ T cell signature. In melanoma, the OBCFA and BOVLCFA pathways were both positively correlated with $CD8^+$ T cell activation. However, in the HCC cohort, the two FAO pathways were negatively correlated with $CD8^+$ T cell signatures, suggesting that FAO pathways may act as immunosuppressive modulators in HCC (Figure 3C). Meta-prognostic analysis of the two pathways in The Cancer Genome Atlas (TCGA) pan-cancer datasets also indicate that higher OBCFA and BOVLCFA activities in TME may be associated with better prognostic outcomes (Figure 3D).

Immuno-metabolic reaction scores indicate higher T cell activity

The immuno-metabolic reaction score (IMRS) was calculated using the following steps (Figure 4A). Briefly, for training cohorts with survival data, both Cox proportional hazards regression and logistic regression were applied, while cohorts without survival data were subjected to logistic regression alone. For each metabolic reaction, univariate Cox or logistic models were established to predict survival outcomes and immunotherapy responses. Meta-analysis was then applied to metabolic reactions related to IRMs in significantly enriched pathways. The final IMRS is the sum of the products by multiplying activities scores and their coefficients in the model for each significant reaction.

Figure 1. Research scheme

(Part 1) GWAS summary data were analyzed using Mendelian randomization (MR) to identify causal relationships between metabolites and immune cells. Significant positive associations, without corresponding negative MR relationships, were selected for metabolic pathway enrichment analysis. (Part 2) Following COMPASS analysis, reactions associated with members of significantly enriched pathways were selected and subjected to Cox proportional hazards regression and logistic model construction in immunotherapy-treated cohorts, based on clinical information. Significant prognostic reactions identified through meta-analysis were selected and used for IMRS calculation. The IMRS was then analyzed for its correlation with cell infiltration, immune-related features, spatial co-localization with immune cells, and prognostic validation in additional cohorts.

Table 1. Immune cell-related metabolites

Selected immune cells	No. of samples	No. of SNPs ($p < 1e{-}5$)	No. of causal related metabolites (IVW $p < 0.05$)	No. of causal related metabolites after reverse MR
$CD4^+$ T cell	3,652	179	68	66
$CD8^+$ T cell	3,652	1,414	65	63
NKT cell	3,653	904	49	48
NK cell	3,653	101	55	55
DC	3,374	705	74	71
Gr-MDSC	1,928	163	58	57
Mo-MDSC	1,927	3,706	49	48
Monocyte	3,727	145	66	61
B cell	3,653	223	57	56
Treg cell	3,405	60	72	70
Tcr γδ cell	3,650	648	61	59
Granulocyte	3,653	167	58	51

DC, dendritic cell; Gr-MDSC, granulocytic myeloid-derived suppressor cell; Mo-MDSC, monocytic myeloid-derived suppressor cell; Tcr γδ, a type of T cell receptor found in γδ T cells.

The significant reactions were categorized into two types: metabolites consuming (C) and metabolites producing (P), based on the position of target metabolites in the reaction equation. Acetyl-carnitine P reactions indicate worse immunotherapy response (HR > 1), while dodecanoyl-coenzyme A C reactions and L-carnitine P reactions are associated with better immunotherapy response (HR < 1) (Figure 4B). The top significant reactions were distinct between immunotherapy responders and non-responders in training and validation sets (Figure 4C). The IMRS was correlated with tumor immune cell infiltration. The results indicated that the IMRS was positively correlated with T cells, $CD8^+$ T cells, dendritic cells (DCs), and B cells in the IMvigor210 and Liu_Melanoma_2019 cohorts (Figure 4D). In the IMvigor210, Rose_2021_GSE176307, and Liu_Melanoma_2019 cohorts, IMRS was also positively correlated with the $CD8^+$ T cell signature, including interferon response, cytotoxicity, cytokine/cytokine receptors, and adhesion, suggesting that higher IMRS may contribute to higher T cell-related antitumor activities in these patients (Figure 4D).

Co-localization of elevated IMRS with $CD8^+$ T effector cell

Spatial transcriptomic data of CRC, CRC liver metastasis (CRLM), and bladder cancer patients treated with immune-checkpoint inhibitors (ICIs) were analyzed for visualizing the co-localization of IMRS and $CD8^+$ T effector cells. For CRC, elevated IMRS was significantly co-localized with $CD8^+$ T effector cells in epithelial cell adhesion molecule-positive ($EPCAM^+$) regions across all samples. Sample colon1 and colon4 exhibited better correlation results than colon2 and colon3, which indicated higher heterogeneity in CRC patients treated with ICIs (Figures 5A and 5B); For CRLM samples, elevated IMRS was significantly co-localized with $CD8^+$ T effector cells, with less individual variance compared to CRC (Figures 5C and 5D). For bladder cancer, elevated IMRS was also positively correlated with $CD8^+$ T effector cells in tumor regions (Figures 5E and 5F).

Pan-cancer prognostic evaluation of IMRS in patients with immunotherapy

To further evaluate the predictive value of IMRS across different cancer types, we utilized a multivariable Cox proportional hazards regression model to analyze the effects of IMRS, tumor stages, and human ethnicity. In the combined melanoma cohorts, IMRS was significantly associated with improved overall survival (OS) outcomes (HR = 0.43, $p < 0.001$), whereas tumor stages were not significantly correlated with OS ($p = 0.144$) (Figure 6A). In the combined bladder cancer cohorts, IMRS was also significantly associated with improved OS outcomes (HR = 0.69, $p < 0.01$). Tumor stages were associated with worse OS outcomes (HR = 2.15, $p < 0.001$), while human race was not a significant predictive factor for OS ($p > 0.05$) (Figure 6B). A Kaplan-Meier (KM) survival analysis of combined melanoma and bladder cancer cohorts showed that elevated IMRS significantly favored better OS ($p < 0.01$) (Figures 6C and 6D). For subgroup analysis, IMvigor210 and Rose_2021 were divided into all-stages groups (M0 and M1x), a metastasis group (M0), and a non-metastasis group (M1x). IMRS was significantly associated with better OS outcomes across all stages including M0 and M1x subgroups (HR < 1, $p < 0.05$) (Figures 6E and 6F). In training set Braun_2020 (renal cell carcinoma [RCC]), IMRS was significantly associated with better OS outcomes across all stages and in the M0 group, but it was not significant in the M1x group ($p = 0.106$) (Figure 6G). In other validation cohorts, IMRS was significantly associated with better OS and progression-free survival (PFS) outcomes in Gide_2019_Melanoma cohorts ($p < 0.05$) (Figures 6H and 6I). IMRS was also significantly associated with better PFS outcomes in Braun_2020 cohorts (HR = 0.66, $p < 0.05$) (Figure 6J).

DISCUSSION

A well-recognized feature of cancer cells is metabolic reprogramming, characterized by the deregulated uptake of glucose and amino acids,

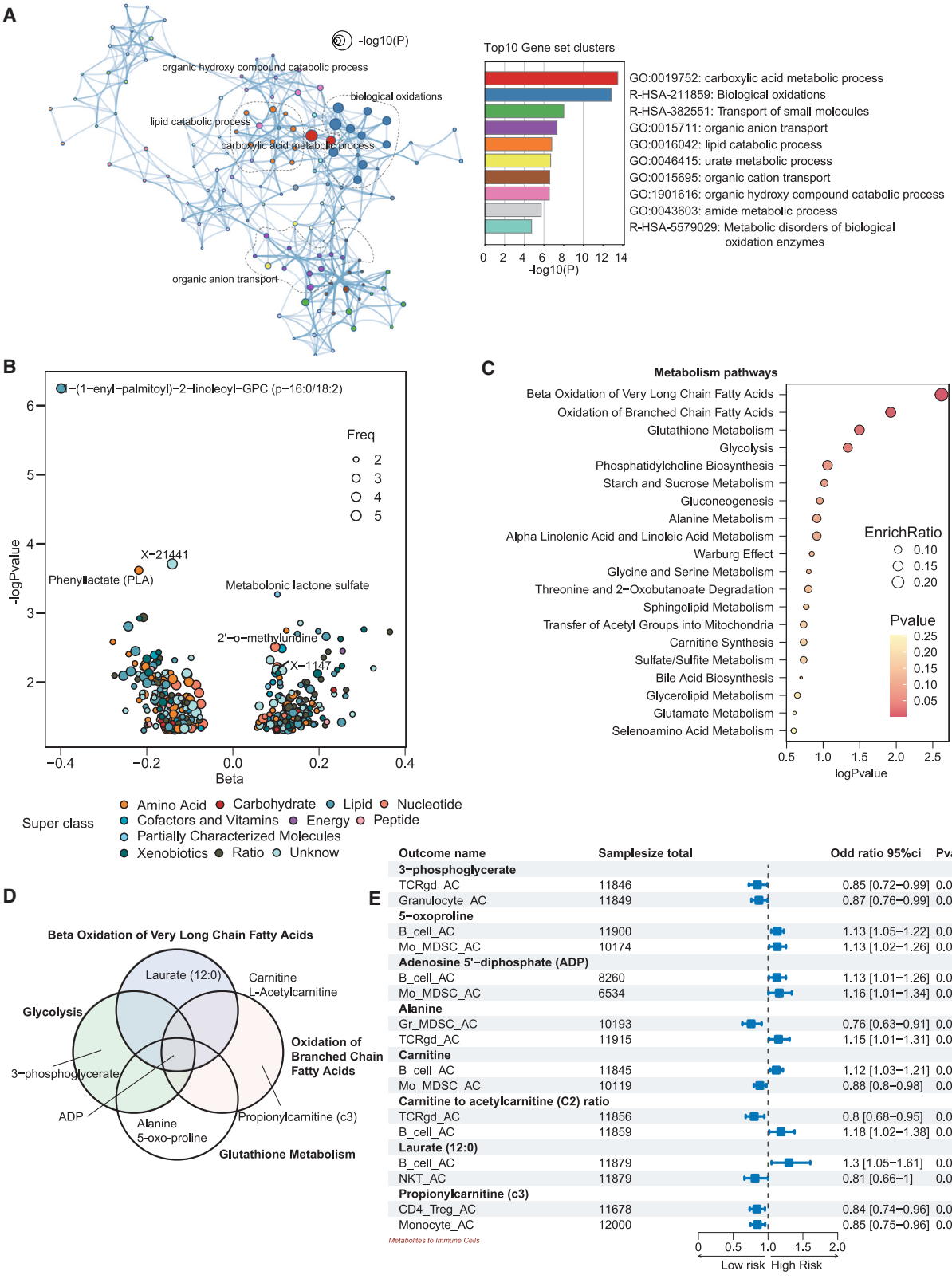

(legend on next page)

as well as elevated FA metabolism, which enhances their plasticity to adapt to extreme environments and metastasis.[14,15] Aberrant metabolite concentrations in the TME have been observed to aid cancer cells in escaping host immune surveillance and surviving.[16–18] For instance, metabolic reprogramming of cancer cells can impair antitumor functions of $CD8^+$ T cells in TME through nutrient competition,[1,19] oxygen deprivation, acidification,[20] or directly signaling modulation via metabolic intermediates.[21] Our findings suggest causal effects of FAO-related metabolites, such as carnitine, dodecanoic acid, and propionylcarnitine, on immune cells in the peripheral blood. These metabolites may also affect immune cell functions in the TME through direct or indirect signaling pathways. Carnitine, which shuttles FAs across cell membranes via carnitine palmitoyl transferase, is a critical cofactor in FAO pathways in almost all cells, including tumor cells.[22] The carnitine palmitoyl transferase family is the rate-limiting FAO enzyme that plays a key role in cancer metabolic adaptation. It is upregulated in most cancer types and promotes cancer survival under metabolic stress,[23,24] potentially leading to reduced carnitine concentration in the TME and serum. Studies have reported decreased serum carnitine levels in various cancers. Carnitine has shown protective effects in cancer patients by inhibiting cancer cell proliferation and enhancing anticancer immune responses.[25] Our results demonstrate that FAO pathways requiring carnitine as a shuttle, along with metabolic reactions producing carnitine in the TME, were associated with better immunotherapy responses, further supporting serum carnitine levels as a potential predictor of cancer therapy outcomes. Dodecanoic acid belongs to the medium-chain FAs class. It has been reported to be associated with the reduced risk of CRC in White participants.[26] However, only a few studies have reported that dodecanoic acid supports the differentiation of pro-inflammatory T helper cells and promotes inflammation.[27] The potential effects of dodecanoic acid in the tumor immune microenvironment require further investigation. These causal metabolites are enriched in FAO pathways, further highlighting the role of FAO pathways in antitumor immunomodulation.

One consequence of metabolic reprogramming in cancer cells is the accumulation of free FAs in the TME.[28–30] Accumulated FAs disrupt mitochondrial function and lead to metabolic exhaustion of intratumoral $CD8^+$ T cells, which would impair the antitumor immune response.[29] Ma et al.[31] also provide evidence that enriched FAs in the TME and CD36 expression on intratumoral $CD8^+$ T effector cells together dampen their antitumor function by reducing cytotoxic cytokine production. The *de novo* FA synthesis pathway, as a source of free FAs in the TME, is emerging as a potential target for improving immunotherapy efficacy.[32] Inhibition of SREBP1, an upstream regulator of lipid synthesis in cancer cells, reduces free FAs in the TME, leading to increased $CD8^+$ T cells and decreased M2-like TAMs during anti-programmed cell death protein 1 (anti-PD-1) therapy.[33] Moreover, the very-long-chain FAO pathway identified in our study is closely associated with ferroptosis, and elevated activity in this pathway may enhance the response to immunotherapy.[33] The FAO pathway, which utilized free FAs in TME may also serve as a potential therapeutic target.[34] FAO and its downstream oxidative phosphorylation pathways are essential for T cells, supporting prolonged and enhanced antitumor functions as well as the formation of memory T cells.[35,36] IMRS in our study was established based on the reactions related to FAO in the TME. Patients with high IMRS in our study exhibited stronger activities in FA transportation to both mitochondria and peroxisome for oxidation. Using spatial transcriptomic data to validate the co-localization of high IMRS area and effector $CD8^+$ T cells in different cancer patients, we may speculate that FAs in the TME are rapidly consumed in high-IMRS individuals, potentially alleviating their immunosuppressive functions. Spatial localization in the TME is essential for the tumor-eliminating function of $CD8^+$ T effector cells. High IMRS in the TME may create a low free FA niche for the immune cells, which could improve immunotherapy efficacy.[37,38] However, spatial co-localization alone is insufficient to prove the causal effects of FA concentration on T cell distribution due to tumor morphological heterogeneity.[39] Spatial sequencing data and methods with higher resolution and broader coverage are required for further validation.[40] Not only the FA concentration but also the classes of FAs and the specific effects of different FAs on TME cell components remain poorly understood. Specific FAs, such as linoleic acid, can improve mitochondrial fitness and promote memory-like phenotypes of $CD8^+$ T cells, enhancing the efficacy of adoptive cell therapy in lymphoma models.[41] Given the heterogeneity among cancer types, further studies are needed to validate the effects of linoleic acid on immunotherapy responses. Considering the complexity of different kinds of FAs, it is necessary to discover new immunotherapy-related FAs and to elucidate the mechanisms underlying the functions of specific FAs and their impact on cancer treatment efficacy.

Many previous studies have highlighted circulating tumor-derived metabolic products (e.g., phospholipids, tryptophan, nicotinamide),[42] immune cells (peripheral immunotypes),[13] proteins (e.g., MBL2, HABP2, CAMP, CETP, CD163 in HCC),[43] and chromatin (e.g., image-based chromatin organization)[44] as diagnostic biomarkers for monitoring cancer progression, metastasis, and treatment efficacy. Still, it is a significant challenge for researchers to determine how peripheral blood multi-omics profiles accurately reflect the true situation in the TME due to limited matched blood-TME investigations.[13,45] Recently, the widespread application of new metabolomic methods to peripheral blood or tumor specimens from patients with various cancers has significantly accelerated the discovery of

Figure 2. Pathway enrichment analysis of metabolites with causal relation to immune cells

(A) Gene set enrichment analysis of SNP-related genes using Metascape. (B) Metabolites with at least two causal relationships with immune cells were selected. The x axis is the β value (nature logarithm of odd ratio, lg(OR)), $\beta > 0$ represents $OR > 1$, and $\beta < 0$ represents $OR < 1$. (C) Metabolite pathway enrichment analysis using Metaboanalyst online tools. Causal related metabolites were significantly enriched in fatty acid oxidation, glycolysis, and glutathione metabolism pathways. (D) Metabolite members of significant enriched pathways. (E) Causal relationship to immune cells of metabolite members of significant enriched pathways.

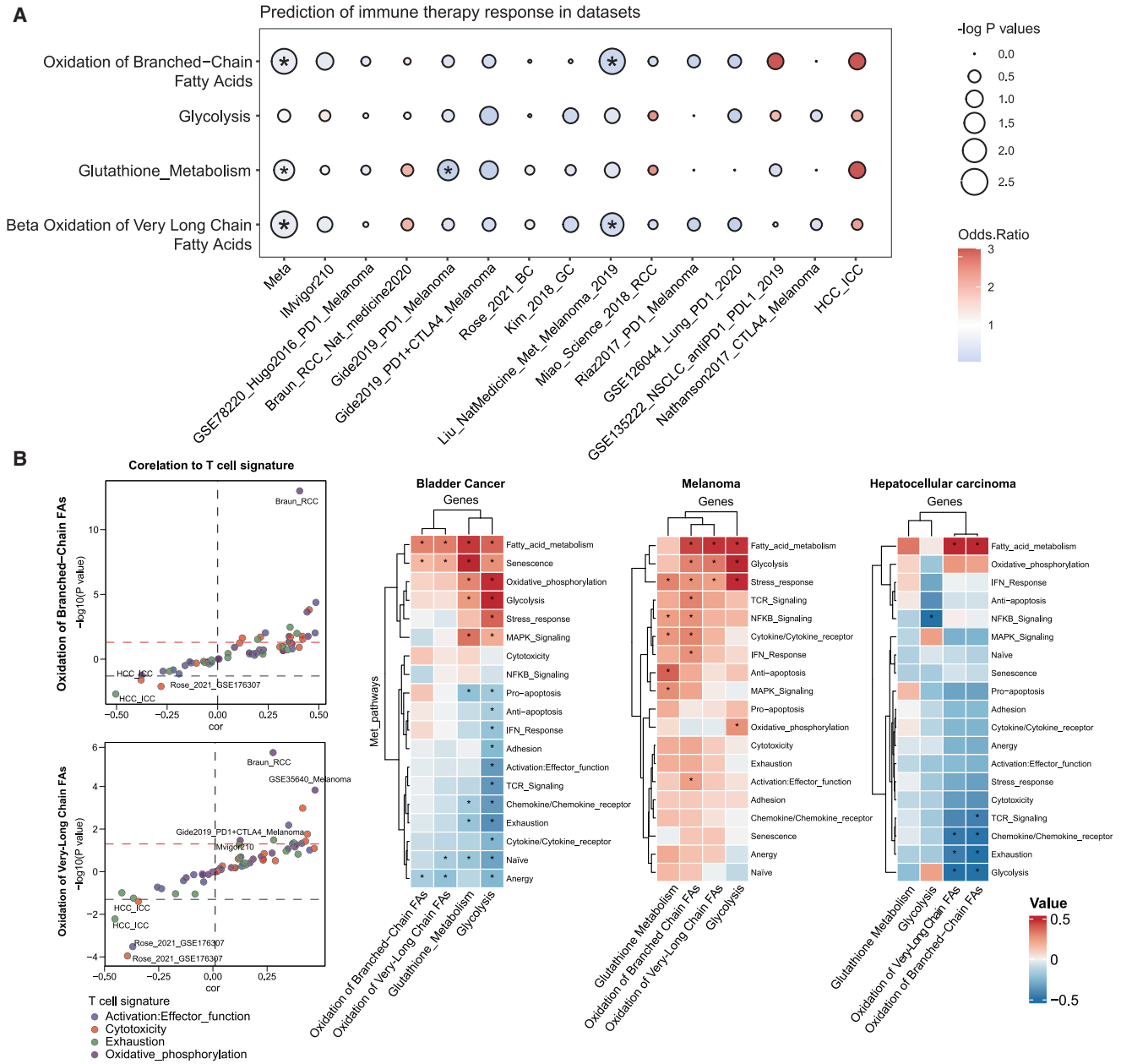

C

Meta-analysis of TCGA pancancer prognosis

Pathways	Cohorts	HR	HR_95ci	pvalue
Oxidation_of_Branched−Chain_Fatty_Acids	33		0.77 [0.71−0.83]	0.000
Beta_Oxidation_of_Very_Long_Chain_Fatty_Acids	33		0.9 [0.83−0.98]	0.010
Glycolysis	33		0.99 [0.92−1.07]	0.887
Glutathione_Metabolism	33		1.01 [0.93−1.09]	0.838

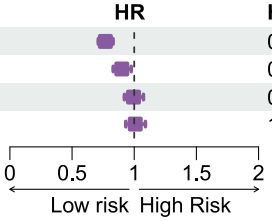

(legend on next page)

new metabolic biomarkers for diagnostic or prognostic purposes.[46–48] Moreover, large-scale clinical trials focusing on blood metabolites for early detection and diagnosis of various cancer types have recently been conducted to develop more accurate diagnostic models.[49,50] However, identifying the causal mechanisms linking blood metabolites to TME cell components remains challenging.[51] Our study established a causal relationship between blood metabolites and blood immune cell profiles, further developing and validating a prognostic model using multi-omics datasets. Two-sample MR analysis utilizes SNP-exposure and SNP-outcome associations from independent genome-wide association studies (GWASs) experiments and combine them into a single causal estimate.[11] With the rapid increase in GWAS datasets on metabolomics and immune cells,[52] large-scale summary statistics have become widely available, enabling MR analyses with significantly greater statistical power. COMPASS is another great tool for translating gene expression data into metabolic reaction data. Using these tools, we developed a novel prognostic model to predict immunotherapy responses with reliable causal effects. Tumor heterogeneity, including variations in stages, locations, and morphological features within the tumor region, can significantly impact the efficacy of immunotherapy.[53,54] Our analysis incorporated tumor stage as a covariate in the prognostic model and identified inconsistencies between early- and late-stage RCC patients. Additional tumor types at various stages should be evaluated to validate the applicability of the prognostic model for new patients in the future. Overall, these advancements could accelerate research on peripheral biomarkers to better reflect the status of the TME.

As metabolic pathways gain increasing attention in cancer therapy, they are emerging as a prominent topic in the development of adjuvants to cancer immunotherapy. Cao et al. utilized lactate oxidase nano-capsules to successfully overcome tumor immunosuppression and enhance the efficacy of immune checkpoint blockade therapy without inducing severe nonspecific toxicity.[55] Numerous preclinical studies have highlighted the potent effects of indoleamine 2,3-dioxygenase 1 inhibitors, which target tryptophan catabolism, in activating antitumor immunity and synergizing with anti-PD-(L)1 therapy.[56] Regarding FAO, Lai et al.[57] demonstrated that dietary elaidic acid, not normal oleic acids, could activate the expression of major histocompatibility complex class I in tumor via NLRC5 and enhance the efficacy of anti-PD-1 therapy in mice. Our findings present new approaches and potential targets for identifying novel peripheral biomarkers to predict immunotherapy responses. However, this study has certain limitations. First, the GWAS samples were derived exclusively from European ancestries, which may limit the generalizability of our conclusions to patients with different genetic backgrounds. Second, the results from MR analysis may be biased due to weak instruments and horizontal pleiotropy; however, F-statistics and statistical tests for pleiotropy may help minimize these biases. Epidemiological studies involving larger populations and diverse ancestries are needed to evaluate the relationships between measured plasma metabolites and immunotherapy efficacy. Additionally, experimental research is required to validate these findings. Third, not all solid tumor patients were included in our studies, meaning the prediction model developed here may not be applicable to all tumor types. In future studies, additional large-scale immunotherapy trials on other cancer types with more samples and detailed information should be included for developing a better prediction model. Despite these limitations, our findings suggest that novel metabolism-related biomarkers and interventions will be rapidly identified through the application of MR, thereby advancing the precise application of immunotherapy across various cancers.

Conclusion

Our study contributes to the growing body of evidence that metabolites are not passive bystanders in cancer progression but active participants in shaping the tumor immune landscape. Further elucidation of these mechanisms could pave the way for therapeutic strategies that integrate metabolic manipulation with immunotherapy, aiming to improve outcomes for patients with solid tumors. Future research in this area is both warranted and essential for advancing cancer therapy.

MATERIALS AND METHODS

Exposure and outcomes data

SNP GWAS summary data for instrument variables was downloaded from previous studies. The summary data of 1,091 metabolites and 309 metabolites' concentration ratios were sourced from an independent GWAS of blood metabolite traits among 8,192 individuals of European ancestry from the Canadian Longitudinal Study on Aging.[58] GWAS data of a total of 731 immune traits were sourced from the GWAS Catalog (accession numbers from GCST0001391 to GCST0002121). The study analyzed 118 absolute cell counts, 389 median fluorescence intensities reflecting surface antigen levels, 32 morphological parameters, and 192 relative cell counts by flow cytometry in 3,757 individuals.[59]

Instrument variables selection and related functional analysis

SNPs that were significantly related to the metabolites were selected as the instrument variables (IVs) according to two thresholds: (1) SNPs less than the genome-wide statistical significance threshold (1×10^{-5}) to serve as IVs and (2) the minor allele frequency threshold of the variants of interest was 0.01. Linkage disequilibrium (LD) clumping was performed with a window size of 10,000 kb to select SNPs that were independently (pairwise LD $R^2 < 0.01$) associated with plasma metabolites at $p < 5 \times 10^{-8}$, as previously described.[60]

Figure 3. Prognostic and correlation analysis of enriched pathways

(A) Prediction of immunotherapy response using four significant enriched pathway scores. (B) Correlation of fatty acid oxidation pathway scores with tumor-related T cell signature in pan-cancer immunotherapy cohorts. Different colors represent types of T cell function signatures. (C) Correlation of four significant enriched pathway scores with $CD8^+$ T cell signatures in IMvigor210, melanoma, and hepatocellular carcinoma treated with immune checkpoint inhibitors. (D) Meta-analysis of significant enriched pathway scores on prognostic prediction in TCGA pan-cancer cohorts.

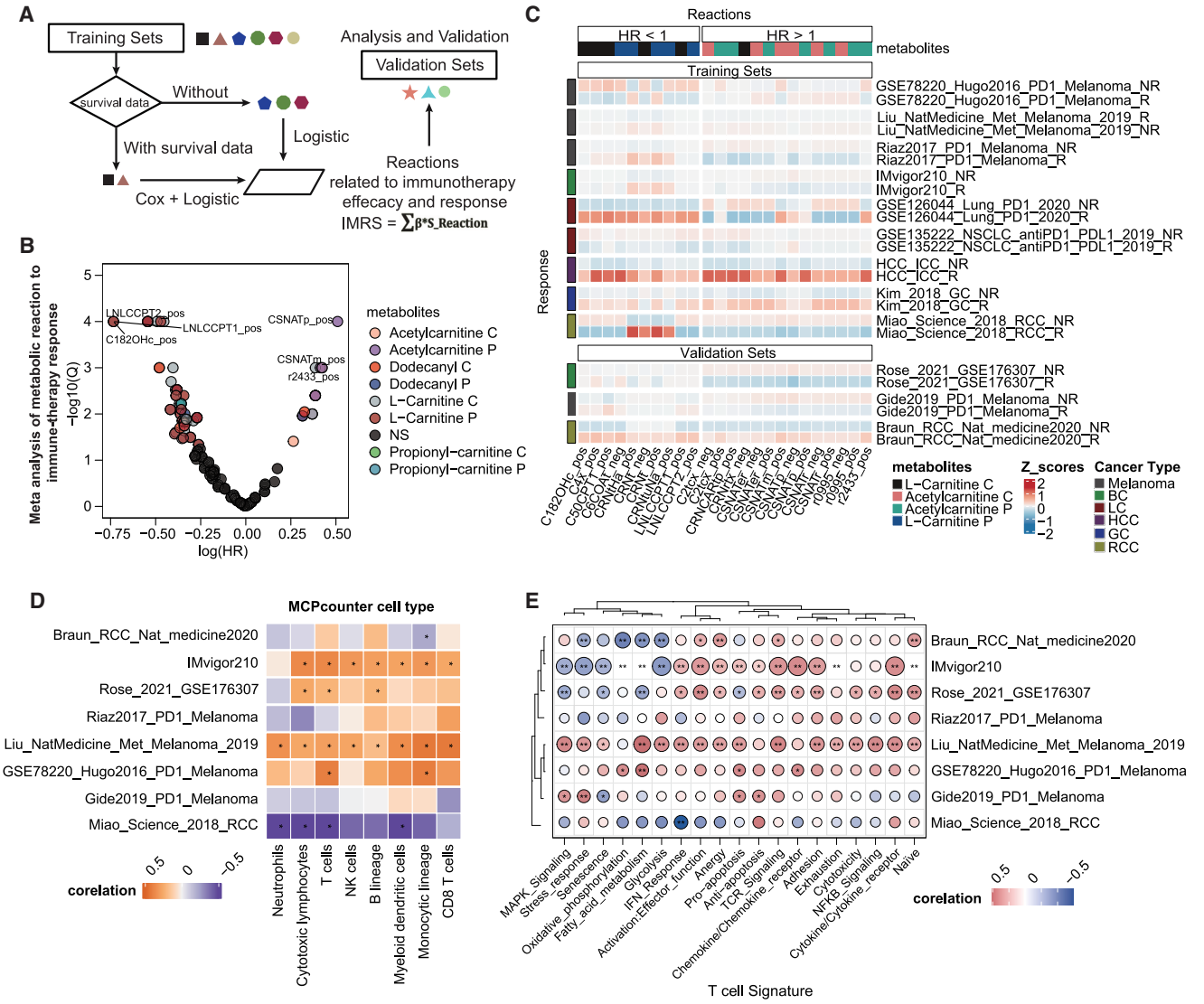

Figure 4. Immunotherapy response prediction and correlation analysis of metabolic reactions

(A) Calculation steps of IMRS. (B) Meta-analysis of metabolic reactions to immunotherapy response. (C) Metabolic reaction score distributions in immunotherapy responders and non-responders. Top 20 metabolic reactions were selected according to their hazard ratio and *p* value. (D) Correlations of metabolic reaction scores with MCP-counter immune cell infiltration scores in pan-cancer immunotherapy cohorts. (E) Correlation analysis of metabolic reaction scores with $CD8^+$ T cell signatures in pan-cancer immunotherapy cohorts.

During the harmonization process, we aligned the alleles to the human genome reference sequence (build 37) and removed ambiguous and duplicated SNPs. After we excluded weak IVs by F-statistic <10 and the Steiger test, metabolites with at least three IVs were eligible for MR analyses. MR-PRESSO and MR-Egger regression tests were applied to monitor the potential horizontal pleiotropy effect. SNPs were sorted in ascending order in terms of their outlier test *p* values and were then removed one by one. The list of SNPs remaining after removing pleiotropic SNPs was used for the subsequent MR analysis. The SNPs selected as IVs were then annotated by Ensembl variant effect predictor tools for related genes and location.[61] For genes with SNPs located on the exon region, gene set enrichment analyses were conducted by Metascape.[62]

MR analysis

Two-sample MR analysis was conducted using the twosampleMR package in R. We employed five different MR methods for features containing multiple IVs, including the inverse-variance weighted (IVW) test, weighted mode, MR-Egger regression, the weighted median estimator, and MR-PRESSO. Within these methods, the IVW method is reported to be more powerful than the others.[63] To avoid type I error, Bonferroni correction was applied to each metabolite

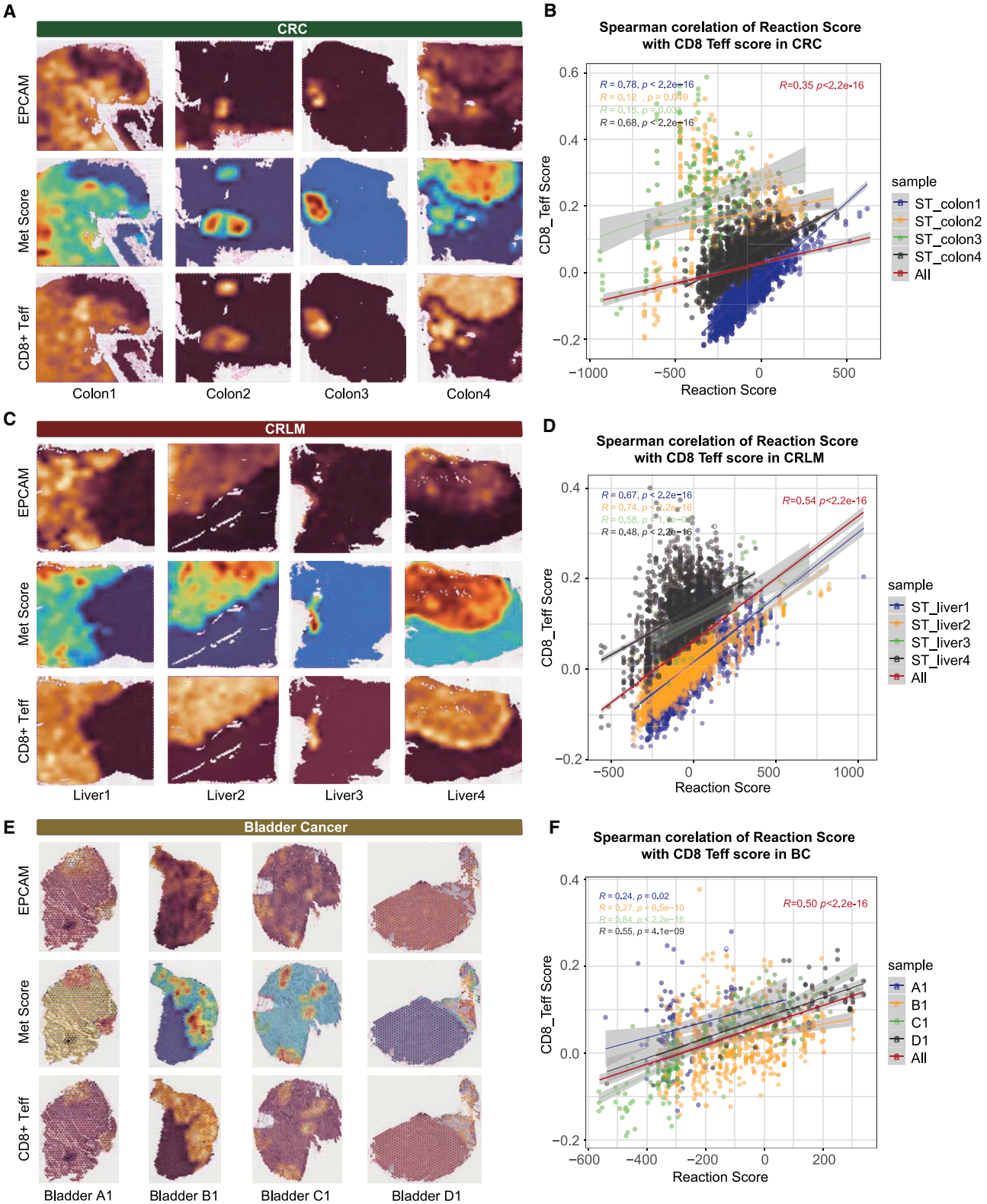

(legend on next page)

to identify significant associations at Bonferroni-corrected $p < 0.05$. To ensure the robustness of findings, complementary analyses were performed using three additional MR approaches. A test was also performed for heterogeneity identification using Cochran's Q statistics in all metabolites. Causal relations results with Q values larger than the number of instruments minus 1 or Q statistics significant at $p < 0.05$ can imply the presence of heterogeneity and be discarded. To confirm whether immune cells have any causal impact on the identified significant metabolites, we also performed a reverse MR analysis (i.e., immune cells as the exposure and the identified causal metabolites as the outcome) using SNPs that are associated with immune cells as IVs. Metabolites with reversed causal relations were filtered out. An MR Steiger directionality test[64] was applied to examine whether exposure was directionally causal for the outcome.

Metabolism enrichment analysis

Each metabolite which has at least two causal relationships with the selected immune cells were collected. They were then subjected to the MetabolAnalyst 6.0 website for metabolite set enrichment analysis (MSEA).[65] First, the metabolite names were compared to the HMDB database to get the correct HMDB identification number according to their structure and molecular formula. Second, the metabolites with unique HMDB identification numbers ("hits") were applied to MSEA of the Small Molecule Pathway Database (SMPDB) metabolic pathways. Finally, the enriched results were visualized by ggplot2 in R.

Pan-cancer immunotherapy datasets

Pan-cancer bulk RNA-seq datasets of patients treated with immunotherapy were acquired in different studies: melanoma,[66–69] bladder cancer,[70,71] RCC,[72,73] lung cancer,[74,75] HCC,[76] and gastric cancer[77] (Figure 1; Table S1). The survival and Response Evaluation Criteria in Solid Tumors (RECIST) data were also acquired in their published information and materials. Gene expression data were normalized and scaled before analysis. For RECIST data, patients with complete response and partial response were considered to be responders, while other patients with stable disease and progressive disease were considered to be non-responders. Cohorts with tumor stages and human ethnicity information were combined according to cancer types for multi-factor Cox proportional hazards regression analysis. IMvigor210, Rose_2021_BC, and Braun_2019_RCC cohorts were divided into subgroups by metastasis stages.

TCGA pan-cancer datasets and tumoral immune cell infiltration analysis

RNA expression data from 33 cancer types were fetched from TCGA database. Metabolic pathway gene sets (protein names) were downloaded from the SMPDB. Pan-cancer tumor-related T cell signature genes were collected from published research about T cell functions related to immunotherapy resistance.[78] These gene sets were utilized for single sample gene set enrichment analysis in TCGA pan-cancer and immunotherapy bulk RNA-seq datasets. MCP-counter[79] was applied to all datasets for tumoral immune cell infiltration analysis.

COMPASS reaction analysis

The COMPASS algorithm was designed for *in silico* modeling of metabolic heterogeneity based on transcriptomic data.[80] We applied COMPASS on spatial transcriptomic and bulk RNA-seq data to characterize metabolic states of tumor samples.

Immunotherapy response prediction and meta-analysis

Univariate logistic regression and univariate Cox proportional hazards regression was performed on each significantly enriched metabolic pathway score and COMPASS reaction to identify the pathway score or reactions that are significantly related to the immunotherapy response in all pan-cancer datasets. Training cohorts with survival data were subject to combined Cox proportional hazards regression and logistic regression; other cohorts without survival data were subject to logistic regression alone. For each metabolic reaction, univariate Cox or logistic regression model was established to predict the survival outcomes and immunotherapy responses. Then, meta-analysis was applied to metabolic reactions that are related to IRMs in significantly enriched pathways. For meta-analysis, nine cohorts (IMvigor210, Hugo_2016_Melanoma, Liu_2019_Melanoma, Riaz_2017_Melanoma, GSE126044, GSE135222, Hsu_2021_HCC, Kim_2018_GC, and Miao_2018_RCC) were selected as the training set. All significant reactions were fitted with random/mixed-effects models by metafor packages in R. Significant reactions after meta-analysis were selected for prognostic signature score calculation. Ultimately, a prognostic signature was constructed by the multiplication of scaled reaction scores and regression coefficient (β) according to the equation:

$$\text{Immune metabolic reaction score (IMRS)} = \beta_1 \times \textit{scaled reaction}_1\ \textit{score} + \beta_2 \times \text{scaled}\ \textit{reaction}_2\ \textit{score} + \ldots + \beta_n \times \textit{scaled reaction}_n\ \textit{score}.$$

Based on the formula, we calculated the signature risk scores of all patients in training and validation cohorts.

Figure 5. Spatial co-localization of metabolic reaction and CD8⁺ T effector cells

A, C and E (left) are the feature plot of EPCAM, IMRS, and CD8⁺ T effector cell score in different cancer types, B, D and F (right) are the correlation plot of IMRS with CD8⁺ T effector cells in tumor sites. (A and B) Spatial feature plot and correlation in CRC. (C and D) Spatial feature plot and correlation in CRLM, related to (A) and (B). (E and F) Spatial feature plot and correlation in bladder cancer.

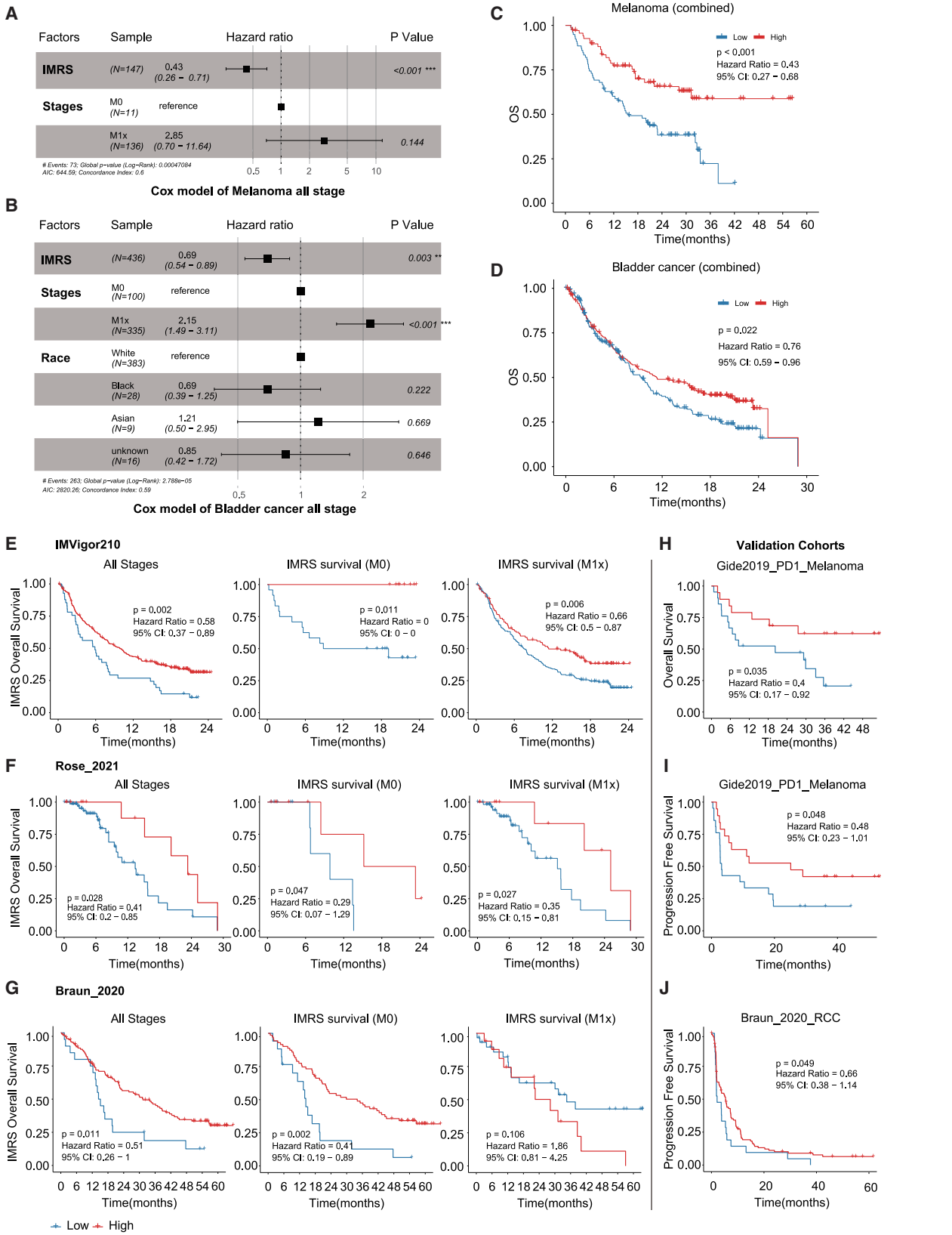

(legend on next page)

Spatial relationship of metabolites to immune cells in tumor sites

Spatial transcriptomic data (10X Visium platform) of CRLM and bladder cancer patients treated with ICIs were collected from two published studies.[81,82] After COMPASS analysis, IMRSs were calculated in all spots on spatial slides. Spatial transcriptome data were analyzed and visualized according to Seurat[83] and SPATA2[84] pipelines. Single-sample gene set variation analyses were also performed to calculate the $CD8^+$ T effector cell signature score in spatial datasets.[81] Tumor cell-specific gene EPCAM were selected for indicating the tumor site on 10X Visium slides. Tumor sites were annotated by visual inspection; IMRSs and $CD8^+$ T effector scores were plotted on tumor sites by SPATA2. Spearman correlations of IMRS with $CD8^+$ T effector scores in all tumor sites of 10X Visium samples were visualized by scatterplot.

Prognostic Cox regression of metabolic reaction score

Patients were classified into high-IMRS and low-IMRS groups for further study according to the optimal cutpoints of the score. A KM analysis was performed to evaluate the statistical differences in survival rate after immunotherapy treatment between the high-IMRS and low-IMRS groups.

DATA AND CODE AVAILABILITY

The data from the original research are available upon request.

ACKNOWLEDGMENTS

This study was funded by the Key Research and Development Program of Zhejiang Province (no. 2019C03021), the National Natural Science Foundation of China (no. 82172362), the Key Laboratory of Precision Medicine in Diagnosis and Monitoring Research of Zhejiang Province (no. 2022E10018), and the Natural Science Foundation of Zhejiang Province under grant no. LQ24H270001. We also express our sincere gratitude to all participants in previously published GWASs and pan-cancer studies.

AUTHOR CONTRIBUTIONS

S.Y., Y.G., and F.Z. contributed to the study design, statistical analysis, and interpretation of the results. S.Y. drafted the manuscript. J.Q.Z. and J.Z. contributed to the writing of the manuscript in English. All authors contributed to the interpretation of the results and critically revised the manuscript. All authors approve the final version of the manuscript and take responsibility for the integrity of the work.

DECLARATION OF INTERESTS

The authors declare no competing interests.

SUPPLEMENTAL INFORMATION

Supplemental information can be found online at https://doi.org/10.1016/j.omton.2025.200933.

REFERENCES

1. Kao, K.-C., Vilbois, S., Tsai, C.-H., and Ho, P.-C. (2022). Metabolic Communication in the Tumour–Immune Microenvironment. Nat. Cell Biol. *24*, 1574–1583. https://doi.org/10.1038/s41556-022-01002-x.

2. DePeaux, K., and Delgoffe, G.M. (2021). Metabolic Barriers to Cancer Immunotherapy. Nat. Rev. Immunol. *21*, 785–797. https://doi.org/10.1038/s41577-021-00541-y.

3. Arner, E.N., and Rathmell, J.C. (2023). Metabolic Programming and Immune Suppression in the Tumor Microenvironment. Cancer Cell *41*, 421–433. https://doi.org/10.1016/j.ccell.2023.01.009.

4. Notarangelo, G., Spinelli, J.B., Perez, E.M., Baker, G.J., Kurmi, K., Elia, I., Stopka, S.A., Baquer, G., Lin, J.-R., Golby, A.J., et al. (2022). Oncometabolite D-2HG Alters T Cell Metabolism to Impair CD8+ T Cell Function. Science *377*, 1519–1529. https://doi.org/10.1126/science.abj5104.

5. Xiao, J., Wang, S., Chen, L., Ding, X., Dang, Y., Han, M., Zheng, Y., Shen, H., Wu, S., Wang, M., et al. (2024). 25-Hydroxycholesterol Regulates Lysosome AMP Kinase Activation and Metabolic Reprogramming to Educate Immunosuppressive Macrophages. Immunity *57*, 1087–1104.e7. https://doi.org/10.1016/j.immuni.2024.03.021.

6. Zhao, L.-Y., Mei, J.-X., Yu, G., Lei, L., Zhang, W.-H., Liu, K., Chen, X.-L., Kołat, D., Yang, K., and Hu, J.-K. (2023). Role of the Gut Microbiota in Anticancer Therapy: from Molecular Mechanisms to Clinical Applications. Signal Transduct. Targeted Ther. *8*, 201–227. https://doi.org/10.1038/s41392-023-01406-7.

7. Jia, D., Wang, Q., Qi, Y., Jiang, Y., He, J., Lin, Y., Sun, Y., Xu, J., Chen, W., Fan, L., et al. (2024). Microbial Metabolite Enhances Immunotherapy Efficacy by Modulating T Cell Stemness in Pan-Cancer. Cell *187*, 1651–1665.e21. https://doi.org/10.1016/j.cell.2024.02.022.

8. Chapman, N.M., and Chi, H. (2024). Metabolic Rewiring and Communication in Cancer Immunity. Cell Chem. Biol. *31*, 862–883. https://doi.org/10.1016/j.chembiol.2024.02.001.

9. Mellman, I., Chen, D.S., Powles, T., and Turley, S.J. (2023). The Cancer-Immunity Cycle: Indication, Genotype, and Immunotype. Immunity *56*, 2188–2205. https://doi.org/10.1016/j.immuni.2023.09.011.

10. Jiménez-Sánchez, A., Cast, O., and Miller, M.L. (2019). Comprehensive Benchmarking and Integration of Tumor Microenvironment Cell Estimation Methods. Cancer Res. *79*, 6238–6246. https://doi.org/10.1158/0008-5472.CAN-18-3560.

11. Sanderson, E., Glymour, M.M., Holmes, M.V., Kang, H., Morrison, J., Munafò, M.R., Palmer, T., Schooling, C.M., Wallace, C., Zhao, Q., and Smith, G.D. (2022). Mendelian Randomization. Nat. Rev. Methods Primers *2*, 6–21. https://doi.org/10.1038/s43586-021-00092-5.

12. Chen, Y., Xie, Y., Ci, H., Cheng, Z., Kuang, Y., Li, S., Wang, G., Qi, Y., Tang, J., Liu, D., et al. (2024). Plasma Metabolites and Risk of Seven Cancers: A Two-Sample Mendelian Randomization Study Among European Descendants. BMC Med. *22*, 90. https://doi.org/10.1186/s12916-024-03272-8.

13. Dyikanov, D., Zaitsev, A., Vasileva, T., Wang, I., Sokolov, A.A., Bolshakov, E.S., Frank, A., Turova, P., Golubeva, O., Gantseva, A., et al. (2024). Comprehensive Peripheral Blood Immunoprofiling Reveals Five Immunotypes with Immunotherapy Response Characteristics in Patients with Cancer. Cancer Cell *42*, 759–779.e12. https://doi.org/10.1016/j.ccell.2024.04.008.

14. Bergers, G., and Fendt, S.-M. (2021). The Metabolism of Cancer Cells during Metastasis. Nat. Rev. Cancer *21*, 162–180. https://doi.org/10.1038/s41568-020-00320-2.

Figure 6. Survival analysis of IMRS in pan-cancer cohorts

(A and B) Multi-factor Cox proportional hazards regression model analysis of IMRS, tumor stages, and patients' ethnicity in combined melanoma and bladder cancer cohorts. (C and D) Kaplan-Meier survival plot of IMRS on OS outcomes in combined melanoma and bladder cancer cohorts. (E) Kaplan-Meier survival plot of OS in IMvigor210 subgroups. (Left) All stages, (center) M0 group, (right) M1x group. (F) Kaplan-Meier survival plot of OS in Rose_2021_BC subgroups. (Left) All stages, (center) M0 group, (right) M1x group. (G) Kaplan-Meier survival plot of OS in Braun_2019 (RCC, training set). (Left) All stages, (center) M0 group, (right) M1x group. (H–J) Kaplan-Meier survival plot of OS and PFS in validation cohorts.

15. Pavlova, N.N., Zhu, J., and Thompson, C.B. (2022). The Hallmarks of Cancer Metabolism: Still Emerging. Cell Metabol. *34*, 355–377. https://doi.org/10.1016/j.cmet.2022.01.007.

16. Xu, S., Chaudhary, O., Rodríguez-Morales, P., Sun, X., Chen, D., Zappasodi, R., Xu, Z., Pinto, A.F.M., Williams, A., Schulze, I., et al. (2021). Uptake of Oxidized Lipids by the Scavenger Receptor CD36 Promotes Lipid Peroxidation and Dysfunction in CD8+ T Cells in Tumors. Immunity *54*, 1561–1577.e7. https://doi.org/10.1016/j.immuni.2021.05.003.

17. Yuan, H., Wu, X., Wu, Q., Chatoff, A., Megill, E., Gao, J., Huang, T., Duan, T., Yang, K., Jin, C., et al. (2023). Lysine Catabolism Reprograms Tumour Immunity through Histone Crotonylation. Nature *617*, 818–826. https://doi.org/10.1038/s41586-023-06061-0.

18. De Martino, M., Rathmell, J.C., Galluzzi, L., and Vanpouille-Box, C. (2024). Cancer Cell Metabolism and Antitumour Immunity. Nat. Rev. Immunol. *24*, 654–669. https://doi.org/10.1038/s41577-024-01026-4.

19. Chang, C.-H., Qiu, J., O'Sullivan, D., Buck, M.D., Noguchi, T., Curtis, J.D., Chen, Q., Gindin, M., Gubin, M.M., van der Windt, G.J.W., et al. (2015). Metabolic Competition in the Tumor Microenvironment Is a Driver of Cancer Progression. Cell *162*, 1229–1241. https://doi.org/10.1016/j.cell.2015.08.016.

20. Brand, A., Singer, K., Koehl, G.E., Kolitzus, M., Schoenhammer, G., Thiel, A., Matos, C., Bruss, C., Klobuch, S., Peter, K., et al. (2016). LDHA-Associated Lactic Acid Production Blunts Tumor Immunosurveillance by T and NK Cells. Cell Metabol. *24*, 657–671. https://doi.org/10.1016/j.cmet.2016.08.011.

21. Elia, I., Rowe, J.H., Johnson, S., Joshi, S., Notarangelo, G., Kurmi, K., Weiss, S., Freeman, G.J., Sharpe, A.H., and Haigis, M.C. (2022). Tumor Cells Dictate Anti-Tumor Immune Responses by Altering Pyruvate Utilization and Succinate Signaling in CD8+ T Cells. Cell Metabol. *34*, 1137–1150.e6. https://doi.org/10.1016/j.cmet.2022.06.008.

22. Qu, Q., Zeng, F., Liu, X., Wang, Q.J., and Deng, F. (2016). Fatty Acid Oxidation and Carnitine Palmitoyltransferase I: Emerging Therapeutic Targets in Cancer. Cell Death Dis. *7*, e2226. https://doi.org/10.1038/cddis.2016.132.

23. Xiong, X., Wen, Y.-A., Fairchild, R., Zaytseva, Y.Y., Weiss, H.L., Evers, B.M., and Gao, T. (2020). Upregulation of CPT1A is Essential for the Tumor-Promoting Effect of Adipocytes in Colon Cancer. Cell Death Dis. *11*, 736. https://doi.org/10.1038/s41419-020-02936-6.

24. Tang, M., Dong, X., Xiao, L., Tan, Z., Luo, X., Yang, L., Li, W., Shi, F., Li, Y., Zhao, L., et al. (2022). CPT1A-Mediated Fatty Acid Oxidation Promotes Cell Proliferation via Nucleoside Metabolism in Nasopharyngeal Carcinoma. Cell Death Dis. *13*, 331. https://doi.org/10.1038/s41419-022-04730-y.

25. Farahzadi, R., Hejazi, M.S., Molavi, O., Pishgahzadeh, E., Montazersaheb, S., and Jafari, S. (2023). Clinical Significance of Carnitine in the Treatment of Cancer: From Traffic to the Regulation. Oxid. Med. Cell. Longev. *2023*, 9328344. https://doi.org/10.1155/2023/9328344.

26. Fan, L., Zhu, X., Chen, Q., Huang, X., Steinwandel, M.D., Shrubsole, M.J., and Dai, Q. (2024). Dietary Medium-Chain Fatty Acids and Risk of Incident Colorectal Cancer in A Predominantly Low-Income Population: A Report from the Southern Community Cohort Study. Am. J. Clin. Nutr. *119*, 7–17. https://doi.org/10.1016/j.ajcnut.2023.10.024.

27. Haghikia, A., Jörg, S., Duscha, A., Berg, J., Manzel, A., Waschbisch, A., Hammer, A., Lee, D.-H., May, C., Wilck, N., et al. (2015). Dietary Fatty Acids Directly Impact Central Nervous System Autoimmunity via the Small Intestine. Immunity *43*, 817–829. https://doi.org/10.1016/j.immuni.2015.09.007.

28. Herber, D.L., Cao, W., Nefedova, Y., Novitskiy, S.V., Nagaraj, S., Tyurin, V.A., Corzo, A., Cho, H.-I., Celis, E., Lennox, B., et al. (2010). Lipid Accumulation and Dendritic Cell Dysfunction in Cancer. Nat. Med. *16*, 880–886. https://doi.org/10.1038/nm.2172.

29. Manzo, T., Prentice, B.M., Anderson, K.G., Raman, A., Schalck, A., Codreanu, G.S., Nava Lauson, C.B., Tiberti, S., Raimondi, A., Jones, M.A., et al. (2020). Accumulation of Long-Chain Fatty Acids in the Tumor Microenvironment Drives Dysfunction in Intrapancreatic CD8+ T Cells. J. Exp. Med. *217*, e20191920. https://doi.org/10.1084/jem.20191920.

30. Su, P., Wang, Q., Bi, E., Ma, X., Liu, L., Yang, M., Qian, J., and Yi, Q. (2020). Enhanced Lipid Accumulation and Metabolism Are Required for the Differentiation and Activation of Tumor-Associated Macrophages. Cancer Res. *80*, 1438–1450. https://doi.org/10.1158/0008-5472.CAN-19-2994.

31. Ma, X., Xiao, L., Liu, L., Ye, L., Su, P., Bi, E., Wang, Q., Yang, M., Qian, J., and Yi, Q. (2021). CD36-Mediated Ferroptosis Dampens Intratumoral CD8+ T Cell Effector Function and Impairs Their Antitumor Ability. Cell Metabol. *33*, 1001–1012.e5. https://doi.org/10.1016/j.cmet.2021.02.015.

32. Röhrig, F., and Schulze, A. (2016). The Multifaceted Roles of Fatty Acid Synthesis in Cancer. Nat. Rev. Cancer *16*, 732–749. https://doi.org/10.1038/nrc.2016.89.

33. Liu, C., Chikina, M., Deshpande, R., Menk, A.V., Wang, T., Tabib, T., Brunazzi, E.A., Vignali, K.M., Sun, M., Stolz, D.B., et al. (2019). Treg Cells Promote the SREBP1-Dependent Metabolic Fitness of Tumor-Promoting Macrophages via Repression of CD8+ T Cell-Derived Interferon-γ. Immunity *51*, 381–397.e6. https://doi.org/10.1016/j.immuni.2019.06.017.

34. Munir, R., Lisec, J., Swinnen, J.V., and Zaidi, N. (2022). Too Complex to Fail? Targeting Fatty Acid Metabolism for Cancer Therapy. Prog. Lipid Res. *85*, 101143. https://doi.org/10.1016/j.plipres.2021.101143.

35. van der Windt, G.J.W., Everts, B., Chang, C.-H., Curtis, J.D., Freitas, T.C., Amiel, E., Pearce, E.J., and Pearce, E.L. (2012). Mitochondrial Respiratory Capacity Is a Critical Regulator of CD8+ T Cell Memory Development. Immunity *36*, 68–78. https://doi.org/10.1016/j.immuni.2011.12.007.

36. Zhou, Z., Zheng, J., Lu, Y., Mai, Z., Lin, Y., Lin, P., Zheng, Y., Chen, X., Xu, R., Zhao, X., and Cui, L. (2024). Optimizing CD8+ T Cell-Based Immunotherapy via Metabolic Interventions: A Comprehensive Review of Intrinsic and Extrinsic Modulators. Exp. Hematol. Oncol. *13*, 103. https://doi.org/10.1186/s40164-024-00575-7.

37. Schenkel, J.M., and Pauken, K.E. (2023). Localization, Tissue Biology and T Cell State — Implications for Cancer Immunotherapy. Nat. Rev. Immunol. *23*, 807–823. https://doi.org/10.1038/s41577-023-00884-8.

38. Zhang, S., Lv, K., Liu, Z., Zhao, R., and Li, F. (2024). Fatty Acid Metabolism of Immune Cells: A New Target of Tumour Immunotherapy. Cell Death Dis. *10*, 39. https://doi.org/10.1038/s41420-024-01807-9.

39. Jena, S.G., Verma, A., and Engelhardt, B.E. (2024). Answering Open Questions in Biology Using Spatial Genomics and Structured Methods. BMC Bioinf. *25*, 291. https://doi.org/10.1186/s12859-024-05912-5.

40. Jiang, J., Liu, Y., Qin, J., Chen, J., Wu, J., Pizzi, M.P., Lazcano, R., Yamashita, K., Xu, Z., Pei, G., et al. (2024). METI: Deep Profiling of Tumor Ecosystems by Integrating Cell Morphology and Spatial Transcriptomics. Nat. Commun. *15*, 7312. https://doi.org/10.1038/s41467-024-51708-9.

41. Nava Lauson, C.B., Tiberti, S., Corsetto, P.A., Conte, F., Tyagi, P., Machwirth, M., Ebert, S., Loffreda, A., Scheller, L., Sheta, D., et al. (2023). Linoleic Acid Potentiates CD8+ T Cell Metabolic Fitness and Antitumor Immunity. Cell Metabol. *35*, 633–650.e9. https://doi.org/10.1016/j.cmet.2023.02.013.

42. Wang, W., Rong, Z., Wang, G., Hou, Y., Yang, F., and Qiu, M. (2023). Cancer Metabolites: Promising Biomarkers for Cancer Liquid Biopsy. Biomark. Res. *11*, 66. https://doi.org/10.1186/s40364-023-00507-3.

43. Xing, X., Cai, L., Ouyang, J., Wang, F., Li, Z., Liu, M., Wang, Y., Zhou, Y., Hu, E., Huang, C., et al. (2023). Proteomics-Driven Noninvasive Screening of Circulating Serum Protein Panels for the Early Diagnosis of Hepatocellular Carcinoma. Nat. Commun. *14*, 8392. https://doi.org/10.1038/s41467-023-44255-2.

44. Challa, K., Paysan, D., Leiser, D., Sauder, N., Weber, D.C., and Shivashankar, G.V. (2023). Imaging and AI Based Chromatin Biomarkers for Diagnosis and Therapy Evaluation from Liquid Biopsies. npj Precis. Oncol. *7*, 135. https://doi.org/10.1038/s41698-023-00484-8.

45. Xu, L., Zou, C., Zhang, S., Chu, T.S.M., Zhang, Y., Chen, W., Zhao, C., Yang, L., Xu, Z., Dong, S., et al. (2022). Reshaping the Systemic Tumor Immune Environment (STIE) and Tumor Immune Microenvironment (TIME) to Enhance Immunotherapy Efficacy in Solid Tumors. J. Hematol. Oncol. *15*, 87. https://doi.org/10.1186/s13045-022-01307-2.

46. Danzi, F., Pacchiana, R., Mafficini, A., Scupoli, M.T., Scarpa, A., Donadelli, M., and Fiore, A. (2023). To Metabolomics and Beyond: A Technological Portfolio to Investigate Cancer Metabolism. Signal Transduct. Targeted Ther. *8*, 137. https://doi.org/10.1038/s41392-023-01380-0.

47. Irajizad, E., Kenney, A., Tang, T., Vykoukal, J., Wu, R., Murage, E., Dennison, J.B., Sans, M., Long, J.P., Loftus, M., et al. (2023). A Blood-Based Metabolomic Signature Predictive of Risk for Pancreatic Cancer. Cell Rep. Med. *4*, 101194. https://doi.org/10.1016/j.xcrm.2023.101194.

48. Sun, C., Wang, A., Zhou, Y., Chen, P., Wang, X., Huang, J., Gao, J., Wang, X., Shu, L., Lu, J., et al. (2023). Spatially Resolved Multi-Omics Highlights Cell-Specific Metabolic Remodeling and Interactions in Gastric Cancer. Nat. Commun. *14*, 2692. https://doi.org/10.1038/s41467-023-38360-5.

49. Wang, Y., An, R., Yu, H., Dai, Y., Lou, L., Quan, S., Chen, R., Ding, Y., Zhao, H., Wu, X., et al. (2024). Largescale Multicenter Study of A Serum Metabolite Biomarker Panel for the Diagnosis of Breast Cancer. iScience *27*, 110345. https://doi.org/10.1016/j.isci.2024.110345.

50. Li, Y., Xu, X., Zeng, C., Qing, B., Liu, L., Song, G., Yu, S., Shao, T., Wei, Q., Wen, H., et al. (2024). Blood Metabolites–Based MCTarg for Multi-Cancer Screening and Clinical Diagnosis. J. Clin. Oncol. *42*, e15028. https://doi.org/10.1200/JCO.2024.42.16_suppl.e15028.

51. Elia, I., and Haigis, M.C. (2021). Metabolites and the Tumour Microenvironment: from Cellular Mechanisms to Systemic Metabolism. Nat. Metab. *3*, 21–32. https://doi.org/10.1038/s42255-020-00317-z.

52. Chen, Y., Lu, T., Pettersson-Kymmer, U., Stewart, I.D., Butler-Laporte, G., Nakanishi, T., Cerani, A., Liang, K.Y.H., Yoshiji, S., Willett, J.D.S., et al. (2023). Genomic Atlas of the Plasma Metabolome Prioritizes Metabolites Implicated in Human Diseases. Nat. Genet. *55*, 44–53. https://doi.org/10.1038/s41588-022-01270-1.

53. Wang, Y., Li, C., Wang, Z., Wang, Z., Wu, R., Wu, Y., Song, Y., and Liu, H. (2022). Comparison Between Immunotherapy Efficacy in Early Non-Small Cell Lung Cancer and Advanced Non-Small Cell Lung Cancer: A Systematic Review. BMC Med. *20*, 426. https://doi.org/10.1186/s12916-022-02580-1.

54. Vitale, I., Shema, E., Loi, S., and Galluzzi, L. (2021). Intratumoral Heterogeneity in Cancer Progression and Response to Immunotherapy. Nat. Med. *27*, 212–224. https://doi.org/10.1038/s41591-021-01233-9.

55. Cao, Z., Xu, D., Harding, J., Chen, W., Liu, X., Wang, Z., Wang, L., Qi, T., Chen, S., Guo, X., et al. (2023). Lactate Oxidase Nanocapsules Boost T Cell Immunity and Efficacy of Cancer Immunotherapy. Sci. Transl. Med. *15*, eadd2712. https://doi.org/10.1126/scitranslmed.add2712.

56. Opitz, C.A., Somarribas Patterson, L.F., Mohapatra, S.R., Dewi, D.L., Sadik, A., Platten, M., and Trump, S. (2020). The Therapeutic Potential of Targeting Tryptophan Catabolism in Cancer. Br. J. Cancer *122*, 30–44. https://doi.org/10.1038/s41416-019-0664-6.

57. Lai, Y., Gao, Y., Lin, J., Liu, F., Yang, L., Zhou, J., Xue, Y., Li, Y., Chang, Z., Li, J., et al. (2024). Dietary Elaidic Acid Boosts Tumoral Antigen Presentation and Cancer Immunity via ACSL5. Cell Metabol. *36*, 822–838.e8. https://doi.org/10.1016/j.cmet.2024.01.012.

58. Surendran, P., Stewart, I.D., Au Yeung, V.P.W., Pietzner, M., Raffler, J., Wörheide, M.A., Li, C., Smith, R.F., Wittemans, L.B.L., Bomba, L., et al. (2022). Rare and Common Genetic Determinants of Metabolic Individuality and Their Effects on Human Health. Nat. Med. *28*, 2321–2332. https://doi.org/10.1038/s41591-022-02046-0.

59. Orrù, V., Steri, M., Sidore, C., Marongiu, M., Serra, V., Olla, S., Sole, G., Lai, S., Dei, M., Mulas, A., et al. (2020). Complex Genetic Signatures in Immune Cells Underlie Autoimmunity and Inform Therapy. Nat. Genet. *52*, 1036–1045. https://doi.org/10.1038/s41588-020-0684-4.

60. Long, Y., Tang, L., Zhou, Y., Zhao, S., and Zhu, H. (2023). Causal Relationship between Gut Microbiota and Cancers: A Two-Sample Mendelian Randomisation Study. BMC Med. *21*, 66. https://doi.org/10.1186/s12916-023-02761-6.

61. McLaren, W., Gil, L., Hunt, S.E., Riat, H.S., Ritchie, G.R.S., Thormann, A., Flicek, P., and Cunningham, F. (2016). The Ensembl Variant Effect Predictor. Genome Biol. *17*, 122. https://doi.org/10.1186/s13059-016-0974-4.

62. Zhou, Y., Zhou, B., Pache, L., Chang, M., Khodabakhshi, A.H., Tanaseichuk, O., Benner, C., and Chanda, S.K. (2019). Metascape Provides a Biologist-Oriented Resource for the Analysis of Systems-Level Datasets. Nat. Commun. *10*, 1523. https://doi.org/10.1038/s41467-019-09234-6.

63. Bowden, J., Davey Smith, G., Haycock, P.C., and Burgess, S. (2016). Consistent Estimation in Mendelian Randomization with Some Invalid Instruments Using a Weighted Median Estimator. Genet. Epidemiol. *40*, 304–314. https://doi.org/10.1002/gepi.21965.

64. Hemani, G., Tilling, K., and Davey Smith, G. (2017). Orienting the Causal Relationship between Imprecisely Measured Traits Using GWAS Summary Data. PLoS Genet. *13*, e1007081. https://doi.org/10.1371/journal.pgen.1007081.

65. Pang, Z., Lu, Y., Zhou, G., Hui, F., Xu, L., Viau, C., Spigelman, A.F., MacDonald, P.E., Wishart, D.S., Li, S., and Xia, J. (2024). Metaboanalyst 6.0: Towards A Unified Platform for Metabolomics Data Processing, Analysis And Interpretation. Nucleic Acids Res. *52*, W398–W406. gkae253. https://doi.org/10.1093/nar/gkae253.

66. Hugo, W., Zaretsky, J.M., Sun, L., Song, C., Moreno, B.H., Hu-Lieskovan, S., Berent-Maoz, B., Pang, J., Chmielowski, B., Cherry, G., et al. (2016). Genomic and Transcriptomic Features of Response to Anti-PD-1 Therapy in Metastatic Melanoma. Cell *165*, 35–44. https://doi.org/10.1016/j.cell.2016.02.065.

67. Riaz, N., Havel, J.J., Makarov, V., Desrichard, A., Urba, W.J., Sims, J.S., Hodi, F.S., Martín-Algarra, S., Mandal, R., Sharfman, W.H., et al. (2017). Tumor and Microenvironment Evolution during Immunotherapy with Nivolumab. Cell *171*, 934–949.e16. https://doi.org/10.1016/j.cell.2017.09.028.

68. Liu, D., Schilling, B., Liu, D., Sucker, A., Livingstone, E., Jerby-Arnon, L., Zimmer, L., Gutzmer, R., Satzger, I., Loquai, C., et al. (2019). Integrative Molecular and Clinical Modeling of Clinical Outcomes to PD1 Blockade in Patients with Metastatic Melanoma. Nat. Med. *25*, 1916–1927. https://doi.org/10.1038/s41591-019-0654-5.

69. Gide, T.N., Quek, C., Menzies, A.M., Tasker, A.T., Shang, P., Holst, J., Madore, J., Lim, S.Y., Velickovic, R., Wongchenko, M., et al. (2019). Distinct Immune Cell Populations Define Response to Anti-PD-1 Monotherapy and Anti-PD-1/Anti-CTLA-4 Combined Therapy. Cancer Cell *35*, 238–255.e6. https://doi.org/10.1016/j.ccell.2019.01.003.

70. Mariathasan, S., Turley, S.J., Nickles, D., Castiglioni, A., Yuen, K., Wang, Y., Kadel, E.E., III, Koeppen, H., Astarita, J.L., Cubas, R., et al. (2018). TGFB Attenuates Tumour Response to PD-L1 Blockade by Contributing to Exclusion of T Cells. Nature *554*, 544–548. https://doi.org/10.1038/nature25501.

71. Rose, T.L., Weir, W.H., Mayhew, G.M., Shibata, Y., Eulitt, P., Uronis, J.M., Zhou, M., Nielsen, M., Smith, A.B., Woods, M., et al. (2021). Fibroblast Growth Factor Receptor 3 Alterations and Response to Immune Checkpoint Inhibition in Metastatic Urothelial Cancer: A Real World Experience. Br. J. Cancer *125*, 1251–1260. https://doi.org/10.1038/s41416-021-01488-6.

72. Braun, D.A., Hou, Y., Bakouny, Z., Ficial, M., Sant' Angelo, M., Forman, J., Ross-Macdonald, P., Berger, A.C., Jegede, O.A., Elagina, L., et al. (2020). Interplay of Somatic Alterations and Immune Infiltration Modulates Response to PD-1 Blockade in Advanced Clear Cell Renal Cell Carcinoma. Nat. Med. *26*, 909–918. https://doi.org/10.1038/s41591-020-0839-y.

73. Miao, D., Margolis, C.A., Gao, W., Voss, M.H., Li, W., Martini, D.J., Norton, C., Bossé, D., Wankowicz, S.M., Cullen, D., et al. (2018). Genomic Correlates of Response to Immune Checkpoint Therapies in Clear Cell Renal Cell Carcinoma. Science *359*, 801–806. https://doi.org/10.1126/science.aan5951.

74. Cho, J.-W., Hong, M.H., Ha, S.-J., Kim, Y.-J., Cho, B.C., Lee, I., and Kim, H.R. (2020). Genome-Wide Identification of Differentially Methylated Promoters and Enhancers Associated with Response to Anti-PD-1 Therapy in Non-Small Cell Lung Cancer. Exp. Mol. Med. *52*, 1550–1563. https://doi.org/10.1038/s12276-020-00493-8.

75. Kim, J.Y., Choi, J.K., and Jung, H. (2020). Genome-Wide Methylation Patterns Predict Clinical Benefit of Immunotherapy in Lung Cancer. Clin. Epigenet. *12*, 119. https://doi.org/10.1186/s13148-020-00907-4.

76. Kudo, M. (2021). Sequential Therapy for Hepatocellular Carcinoma after Failure of Atezolizumab plus Bevacizumab Combination Therapy. Liver Cancer *10*, 85–93. https://doi.org/10.1159/000514312.

77. Kim, S.T., Cristescu, R., Bass, A.J., Kim, K.-M., Odegaard, J.I., Kim, K., Liu, X.Q., Sher, X., Jung, H., Lee, M., et al. (2018). Comprehensive Molecular Characterization of

Clinical Responses to PD-1 Inhibition in Metastatic Gastric Cancer. Nat. Med. *24*, 1449–1458. https://doi.org/10.1038/s41591-018-0101-z.

78. Chu, Y., Dai, E., Li, Y., Han, G., Pei, G., Ingram, D.R., Thakkar, K., Qin, J.-J., Dang, M., Le, X., et al. (2023). Pan-Cancer T Cell Atlas Links A Cellular Stress Response State to Immunotherapy Resistance. Nat. Med. *29*, 1550–1562. https://doi.org/10.1038/s41591-023-02371-y.

79. Becht, E., Giraldo, N.A., Lacroix, L., Buttard, B., Elarouci, N., Petitprez, F., Selves, J., Laurent-Puig, P., Sautès-Fridman, C., Fridman, W.H., and de Reyniès, A. (2016). Estimating the Population Abundance of Tissue-Infiltrating Immune and Stromal Cell Populations Using Gene Expression. Genome Biol. *17*, 218. https://doi.org/10.1186/s13059-016-1070-5.

80. Wagner, A., Wang, C., Fessler, J., DeTomaso, D., Avila-Pacheco, J., Kaminski, J., Zaghouani, S., Christian, E., Thakore, P., Schellhaass, B., et al. (2021). Metabolic Modeling of Single Th17 Cells Reveals Regulators of Autoimmunity. Cell *184*, 4168–4185.e21. https://doi.org/10.1016/j.cell.2021.05.045.

81. Wu, Y., Yang, S., Ma, J., Chen, Z., Song, G., Rao, D., Cheng, Y., Huang, S., Liu, Y., Jiang, S., et al. (2022). Spatiotemporal Immune Landscape of Colorectal Cancer Liver Metastasis at Single-Cell Level. Cancer Discov. *12*, 134–153. https://doi.org/10.1158/2159-8290.CD-21-0316.

82. Gouin, K.H., Ing, N., Plummer, J.T., Rosser, C.J., Ben Cheikh, B., Oh, C., Chen, S.S., Chan, K.S., Furuya, H., Tourtellotte, W.G., et al. (2021). An N-Cadherin 2 Expressing Epithelial Cell Subpopulation Predicts Response to Surgery, Chemotherapy and Immunotherapy in Bladder Cancer. Nat. Commun. *12*, 4906. https://doi.org/10.1038/s41467-021-25103-7.

83. Satija, R., Farrell, J.A., Gennert, D., Schier, A.F., and Regev, A. (2015). Spatial Reconstruction of Single-Cell Gene Expression Data. Nat. Biotechnol. *33*, 495–502. https://doi.org/10.1038/nbt.3192.

84. Kueckelhaus, J., Frerich, S., Kada-Benotmane, J., Koupourtidou, C., Ninkovic, J., Dichgans, M., Beck, J., Schnell, O., and Heiland, D.H. (2024). Inferring Histology-Associated Gene Expression Gradients in Spatial Transcriptomic Studies. Nat. Commun. *15*, 7280. https://doi.org/10.1038/s41467-024-50904-x.